UNIVERSITAT DE BARCELONA

Estudi de dos mecanismes moleculars implicats en l'expressió local d'mRNAs en plasticitat sinàptica

Raül Ortiz Hernández

Cell Reports

Report

Recruitment of Staufen2 Enhances Dendritic Localization of an Intron-Containing *CaMKIIα* mRNA

Graphical Abstract

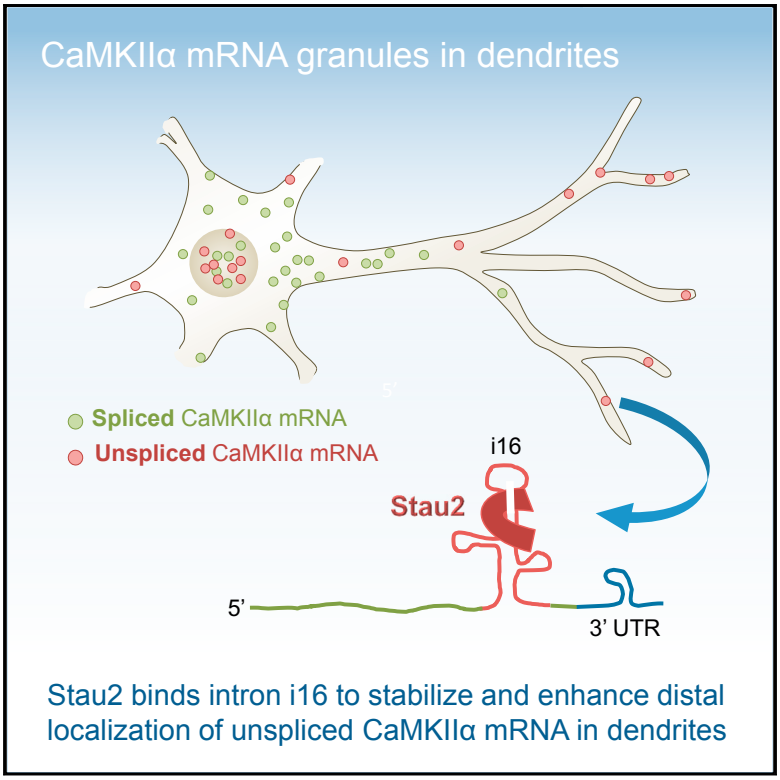

Stau2 binds intron i16 to stabilize and enhance distal localization of unspliced CaMKIIα mRNA in dendrites

Highlights

- *CaMKIIα* mRNA containing intron i16 is present in synaptoneurosomes and RNA granules
- Synaptic activity modulates the presence of i16-containing mRNA in synaptoneurosomes
- Intron 16 is associated with components of RNA granules in dendrites
- Stau2 interacts with i16-containing mRNA and enhances its distal dendritic localization

Authors

Raúl Ortiz, Maya V. Georgieva, Sara Gutiérrez, Neus Pedraza, Sandra M. Fernández-Moya, Carme Gallego

Correspondence

cggbmc@ibmb.csic.es

In Brief

Ortiz et al. have found that a subset of the total *CaMKIIα* mRNA population retains an intron in dendrites. Staufen2 interacts with this intron and enhances the distal dendritic localization of unspliced *CaMKIIα* mRNA. These findings suggest that intron retention could be a mechanism to modulate dendritic localization of synaptic mRNAs.

Ortiz et al., 2017, Cell Reports *20*, 13–20
July 5, 2017
http://dx.doi.org/10.1016/j.celrep.2017.06.026

CellPress

Cell Reports
Report

Recruitment of Staufen2 Enhances Dendritic Localization of an Intron-Containing *CaMKIIα* mRNA

Raúl Ortiz,[1,4] Maya V. Georgieva,[1,4] Sara Gutiérrez,[1] Neus Pedraza,[2] Sandra M. Fernández-Moya,[3] and Carme Gallego[1,5,*]
[1]Molecular Biology Institute of Barcelona (IBMB-CSIC), 08028 Barcelona, Catalonia, Spain
[2]Institut de Recerca Biomèdica de Lleida (IRBLleida), Departament de Ciències Mèdiques Bàsiques, Universitat de Lleida, 25198 Lleida, Catalonia, Spain
[3]Biomedical Center, Division of Anatomy and Cell Biology, Ludwig Maximilians University, 82152 Planegg-Martinsried, Germany
[4]These authors contributed equally
[5]Lead Contact
*Correspondence: cggbmc@ibmb.csic.es
http://dx.doi.org/10.1016/j.celrep.2017.06.026

SUMMARY

Regulation of mRNA localization is a conserved cellular process observed in many types of cells and organisms. Asymmetrical mRNA distribution plays a particularly important role in the nervous system, where local translation of localized mRNA represents a key mechanism in synaptic plasticity. *CaMKIIα* is a very abundant mRNA detected in neurites, consistent with its crucial role at glutamatergic synapses. Here, we report the presence of *CaMKIIα* mRNA isoforms that contain intron i16 in dendrites, RNA granules, and synaptoneurosomes from primary neurons and brain. This subpopulation of unspliced mRNA preferentially localizes to distal dendrites in a synaptic-activity-dependent manner. Staufen2, a well-established marker of RNA transport in dendrites, interacts with intron i16 sequences and enhances its distal dendritic localization, pointing to the existence of intron-mediated mechanisms in the molecular pathways that modulate dendritic transport and localization of synaptic mRNAs.

INTRODUCTION

The targeting of mRNAs to dendrites requires the recognition of *cis*-localization elements (LEs) by RNA-binding proteins (RBPs) (Ule and Darnell, 2006), usually as part of a larger complex of ribonucleoproteins (RNPs), also known as neuronal RNA granules (Buchan, 2014; Kiebler and Bassell, 2006). Several recent studies have consolidated the notion that many introns are actively retained in mature mRNAs (Bell et al., 2010; Wong et al., 2013; Yap et al., 2012). To investigate the contribution of intron retention to cytoplasmic mRNA distribution, we decided to perform an intron disequilibrium analysis in dendritically localized mRNAs. Since *CaMKIIα* has a central role in neuronal signaling (Hell, 2014) and recent genome-wide studies have shown intronic sequences retained in *CaMKIIα* mRNAs from neuronal samples (Braunschweig et al., 2014), we decided to focus our study on this important dendritic transcript. Here, we demonstrate the presence of *CaMKIIα* mRNA molecules retaining intron i16 in dendrites, RNA granules, and synaptoneurosomal fractions, the presence of i16 being predominant in distal dendrites depending on synaptic activation. Our study shows that synaptic activation downregulates i16-containing *CaMKIIα* mRNA in a mechanism that depends on its translation. Notably, this i16-containing transcript specifically interacts with Staufen2 (Stau2), a well-known RBP involved in the targeting of mRNAs to neuronal dendrites (Heraud-Farlow and Kiebler, 2014). As Stau2 is important in enhancing dendritic localization of intron-i16-containing *CaMKIIα* mRNA, our findings suggest that intron retention could have key roles in the assembly and stabilization of an mRNA subpopulation to fine-tune CaMKIIα activity at synapses.

RESULTS

Intron Disequilibrium Analysis of *CaMKIIα*

To investigate the contribution of intron retention in modulating *CaMKIIα* mRNA function, we performed an intron disequilibrium analysis with probes located at exon-intron junctions (Figure 1A). We initially focused on two introns (i14 and i16) previously shown to be involved in intron retention and alternative splicing (Braunschweig et al., 2014), while i9 and i11 were used as controls. Using RNA from embryonic day 17 (E17) cortical cultures and adult mouse brain, we found that i16-containing transcripts were the most abundant compared with other intron-containing transcripts in total cell extracts and synaptoneurosomes from cortical cells and brain (Figures 1B, 1D, S1A, and S1B). Sequences around both the 5′ and 3′ splice sites of intron i16 were similarly enriched in samples from mouse brain (Figure S1D), making alternative transcription termination events within intron i16 unlikely. We also observed an increased presence of i14-containing transcripts in embryonic samples, cortical and hippocampal cells obtained from 17-day embryos, compared to adult brain, suggesting a putative role of i14 during development (Figures 1B, 1D, S1A, and S1B). Next, we extended the analysis to all *CaMKIIα* introns in synaptoneurosomes from cortical cultures and RNA granules from brain (Figures 1C and 1E). In both fractions, we found higher levels of i16-containing transcript compared with other intron-containing RNAs. Our data are consistent with a recent high-throughput RNA-sequencing analysis (Braunschweig et al., 2014) that shows i16

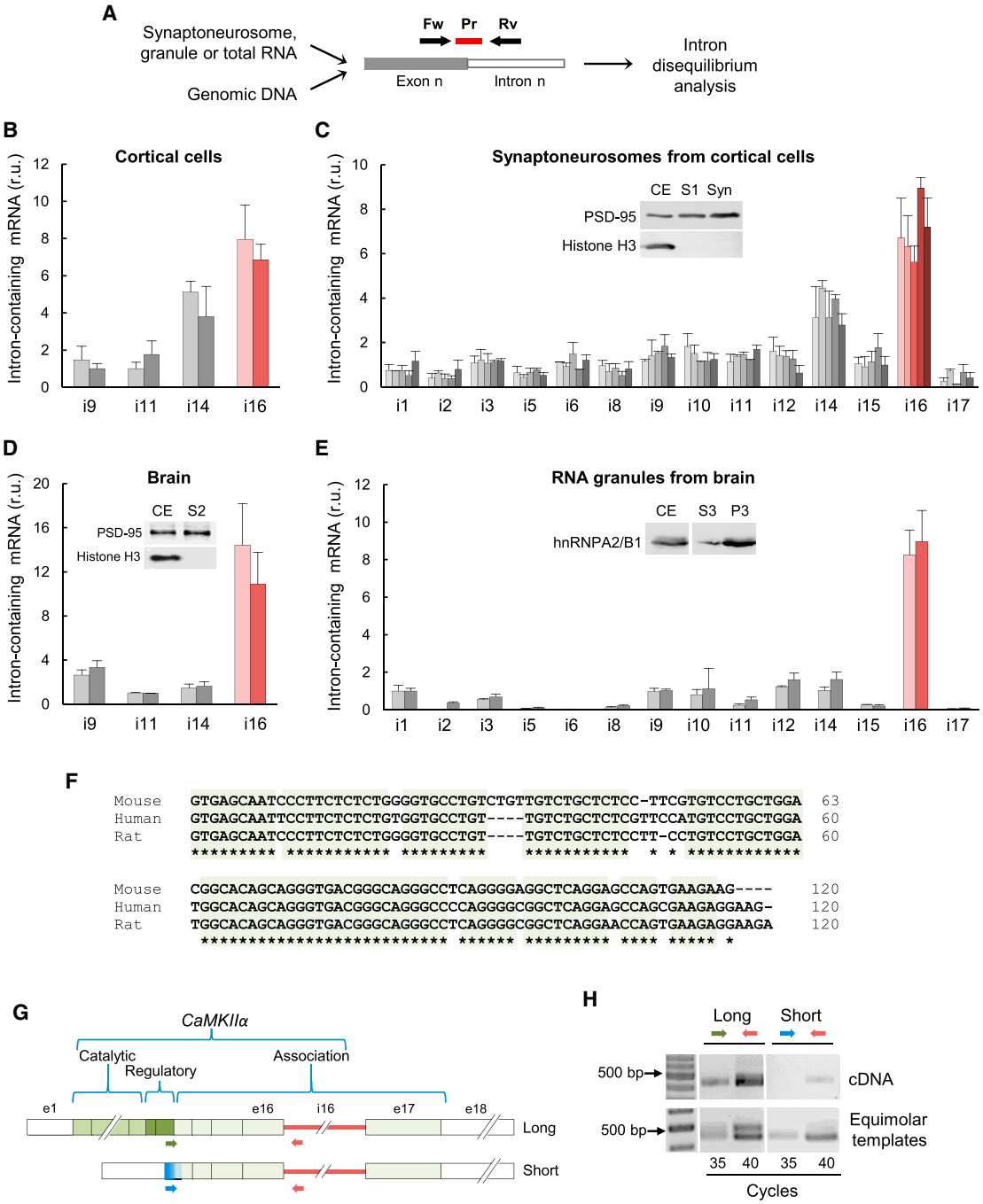

Figure 1. *CaMKIIα* mRNA Containing Intron i16 Is Present in Synaptoneurosomes and RNA Granules

(A) Schematic of the intron disequilibrium analysis by quantitative RT-PCR (qRT-PCR).

(B–E) Intron disequilibrium by qRT-PCR analysis. All probes were made relative to genomic DNA to correct for differences in primer efficiency. RNA was obtained from (B) 14 days in vitro (DIV) cortical cell culture cytoplasmatic fraction, (C) synaptoneurosome fraction from cortical cells (obtained by Percoll gradient), (D) nucleus-free mouse brain extract, and (E) RNA granule fraction from mouse brain. Each bar corresponds to an independent experiment and represents the relative mean value from three independent qRT-PCR measurements. Confidence limits (α = 0.05) are also shown. The boxes in (C)–(E) show representative western blots of PSD-95, histone H3, and hnRNPA2/B1 from total cell extracts (CE), input (S1–S3), or synaptoneurosomes (Syn) and RNA granule (P3) fractions.

(F) Sequence alignment of the first 120 nt of *CaMKIIα* intron i16 from mouse, human, and rat.

(G) Scheme of *CaMKIIα* mRNA long (L) and short (S) isoforms. Colored arrows represent primers used for semiquantitative PCR analysis.

(H) Semiquantitative PCR using cDNA from mouse nucleus-free brain extracts. Primer efficiency was assessed by equimolar template amplification.

retention in samples of human and mouse neuronal origin, being particularly high in Neuro-2a neuroblastoma cells, a finding consistent with our observations (Figure S1C). Another study in rat isolated dendrites also showed cytoplasmic retention of intron i10 (the rat equivalent to mouse i16), although with a moderate p value (0.076) (Buckley et al., 2011).

Sequence alignment revealed that the first 120 nt of intron i16 are 86.3% identical when comparing rodents and humans (Figure 1F), which indicates an extremely high conservation compared to other intronic sequences (Figure S1E). In contrast, amino acid sequences that arise from the 5′ end of i16 are not particularly conserved (Figure S1F), suggesting conserved mechanisms at the transcript level. *CaMKIIα* has two main mRNA isoforms in mice, a long isoform that encodes the whole *CaMKIIα* protein and a short isoform that only includes the C-terminal association domain responsible for assembly of *CaMKIIα* subunits into large multimers. To determine whether i16 is retained in long or short *CaMKIIα* transcript isoforms, we performed a semiquantitative PCR analysis using cDNA from mouse nucleus-free brain extracts (Figure 1D, inset, fraction S2) and found that i16 is mainly retained in the long isoform (Figures 1G and 1H).

Subcellular Localization and Stimulation-Mediated Downregulation of i16-Containing *CaMKIIα* mRNA

We used high-resolution fluorescent in situ hybridization (FISH) to study the localization of i16 transcripts in hippocampal neurons and designed a software plugin (see Experimental Procedures) to quantify foci fluorescence and localization in soma and dendrites. As previously observed (Cajigas et al., 2012), mature *CaMKIIα* mRNAs are very abundant in both soma and dendrites as detected with an exonic probe (Figures S2A–S2C). Notably, the i16 probe produced foci with similar fluorescence intensity when compared to the exonic probe, although at a much lower number. We observed ~15% of co-localization between the two probe sets, which increased to ~40% after 3 min of pepsin treatment (Figure S2D), suggesting that both RNA target sequences are present in the same RNA molecule but masked by a proteinaceous complex as previously described for other dendritic mRNAs (Buxbaum et al., 2014). To facilitate the quantification of dendritic mRNAs, we used microfluidic chambers that compartmentalize soma and neurites and, using this approach, we observed a gradient distribution pattern throughout the somatodendritic compartment for both exonic and intronic foci (Figure 2A). Overexposed Map2 signal shows that both exonic and intron16 foci are present in dendrites (Figure 2B). The i16-containing mRNA represented 3.7% ± 0.33% of the total *CaMKIIα* mRNAs in the somatic cytoplasm. Interestingly, our analysis showed that the percentage of i16-unspliced versus spliced isoforms increased with dendritic distance reaching 28.4% in distal dendrite segments (>200 μm) (Figure 2C).

If i16-containing mRNA is a component of RNA granules, synaptic stimulation might be expected to alter its levels in dendrites. We found that either BDNF or NMDA stimulation produced a significant decrease in i16-containing mRNA by both qRT-PCR in functional synaptoneurosomes (Figure 2D) and high-resolution FISH in hippocampal neurons (Figure 2E). Notably, the BDNF effect was abolished by cycloheximide (Figure 2F), a protein synthesis inhibitor, indicating that downregulation of intron containing mRNA upon stimulation depends on translation as it has been reported for transcripts that are degraded by the mRNA nonsense-mediated decay (NMD) pathway, such as the Arc mRNA (Figure S2E). On the contrary, spliced *CaMKIIα* mRNA levels were not affected by BDNF treatment (Figure 2G). These results point to a specific action of BDNF in the downregulation of i16-containing mRNA.

Intron 16 Interacts with Components of RNA Granules in Dendrites

Since the i16-containing mRNA isoform is differentially localized to distal dendrites, we decided to test whether intron i16 would share interactors with the fully spliced *CaMKIIα* mRNA. To test this possibility, we performed an RNA immunoprecipitation (RIP) analysis in Neuro-2a cells using the MS2 tagging system. While RIP efficiencies of i16 and control ZsGreen-fusion RNAs were similar (Figure S3A), we found that *CaMKIIα* mRNA was significantly enriched in the i16 RIP compared to control (Figure 3A), suggesting that i16-unspliced and spliced *CaMKIIα* mRNAs would share protein interactors. In addition, we found that neurons overexpressing intron i16 displayed a substantially higher number of dendritic *CaMKIIα* mRNA foci (~2-fold) compared to control neurons (Figure 3B and 3C). Since the i16-containing construct does not contain the *CaMKIIα* 3′ UTR, shared protein interactors would depend on specific LEs present in intron i16, as reported for others introns (Buckley et al., 2011). Alternatively, if the increased numbers of dendritic *CaMKIIα* mRNA foci contain i16, our data would point to protein interactions bridging i16-containing mRNA molecules.

Staufen (Stau) proteins belong to a family of RBPs that are critical for targeting specific mRNA in neurons (Heraud-Farlow and Kiebler, 2014; Monshausen et al., 2004; Tang et al., 2001). Given that dendritic *CaMKIIα* mRNA has been associated with Stau2-RNPs (Fritzsche et al., 2013; Jeong et al., 2007), we investigated whether intron i16 could interact with Stau2. Co-expression of exogenous FLAG-Stau2 and ZsGreen fused to intron i16 showed significant enrichment of i16 sequences in the Stau2 immunoprecipitates (IPs) compared to other well-known RBPs (Figure 3D and S3B). Moreover, this enrichment was not obtained with a non-retained intron such as i9 (Figure 3E). Next, we tried to confirm the interaction at endogenous level in brain extracts using two specific antibodies against Stau1 and Stau2. In agreement with overexpression experiments, we found that i16-containing mRNA was specifically enriched in the Stau2 IP compared to control IP and Stau1 IP samples (Figure 3F). Of the different splicing variants of Stau2 (Monshausen et al., 2004) (see input sample in Figure S3C), our IPs (Stau2-IP) mostly contained the largest isoforms, which have an extended C-terminal domain that might interact with a greater variety of RNA granule components than the shorter isoforms (Miki et al., 2011). We also corroborated the endogenous interaction between intron i16 and Stau2 in cortical neurons (Figure S3D), indicating that this interaction occurs in different neuronal models.

Staufen 2 Enhances Stabilization and Dendritic Localization of *CaMKIIα* i16-Containing Transcripts

To elucidate the role of Stau2 in the regulation of i16-containing *CaMKIIα* mRNA in primary neurons, we investigated the impact

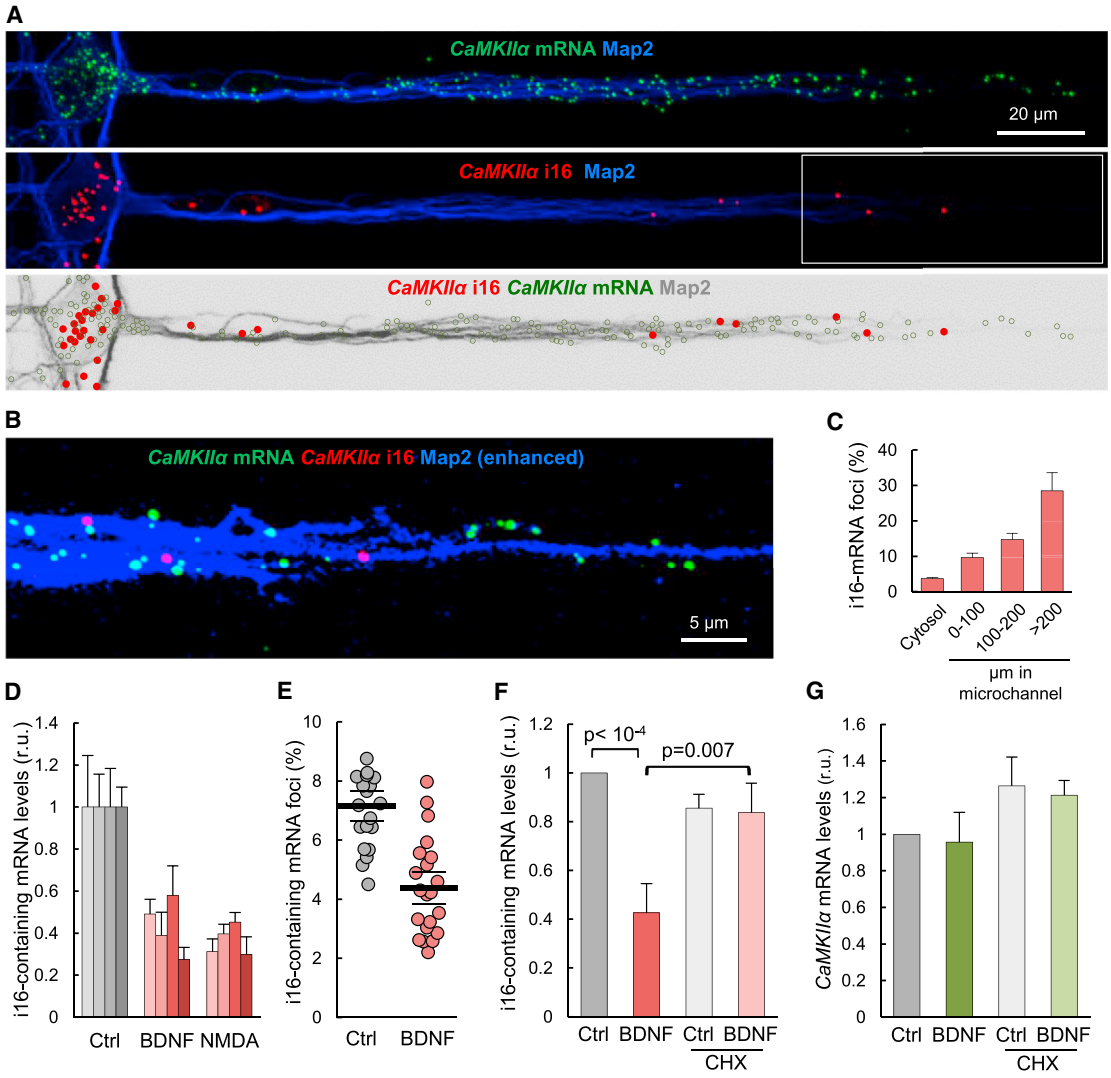

Figure 2. Single-Molecule-Level Localization of i16-Containing *CaMKIIα* mRNA in Dendrites of Hippocampal Neurons and Modulation by Synaptic Activity

(A) Hippocampal cells were seeded in microfluidic chambers in order to isolate dendrites from cell bodies. At 14 DIV, chambers were removed from coverslips and FISH was performed using custom *View*RNA probes against intron i16 (red) or exonic (green) *CaMKIIα* sequences. Dendrites were decorated with an αMap2 antibody (blue). The bottom panel shows identified foci in the red and green channels with the aid of FociJ software. Image shows the first 220 μm of the microchannel as well as part of the main channel where somas and nuclei can be observed.

(B) Detail of white box in (A). The Map2 signal (blue) has been digitally enhanced to show that both exonic and intron16 foci are present in Map2-positive dendrites.

(C) Quantification of the FISH experiment in (A). Percentage of intronic (n = 515) relative to exonic (n = 3,997) foci in cytosol and at different distances in dendrite are shown. Confidence limits (α = 0.05) are also indicated.

(D) Functional synaptoneurosomes were obtained from adult brain cortex by Percoll gradient and stimulated for 30 min with either 200 ng/ml BDNF or 50 μg/ml NMDA. Intron-16-containing mRNA levels relative to *CaMKIIα* were analyzed by qRT-PCR. Each bar stands for an independent experiment and represents mean values from three qRT-PCR measurements made relative to control. Confidence limits (α = 0.05) for the mean are also shown.

(E) Hippocampal cells (14 DIV) were treated with vehicle or 200 ng/ml BDNF for 30 min and analyzed by FISH as in (A). Percentages of intronic relative to exonic foci in dendrites of confluent culture (n = 20 images, neuronal somas were omitted for quantification) are plotted. Mean values (thick horizontal lines) and confidence limits (α = 0.05, thin horizontal lines) for the mean are also shown.

(F) Cortical cell cultures (18 DIV) were treated with actinomycin D (10 μg/ml) for 1 hr prior to stimulation with BDNF 200 ng/ml or vehicle for 30 min. Where indicated, cycloheximide was added to 25 μg/ml 5 min before BDNF. After stimulation, synaptoneurosomal fractions were obtained by filtration and used to quantify i16-containing mRNA levels relative to *Gapdh* mRNA by qRT-PCR. Mean (n = 3) and SEM values are shown.

(G) *CaMKIIα* mRNA levels were measured in synaptoneurosomal fractions as in (F).

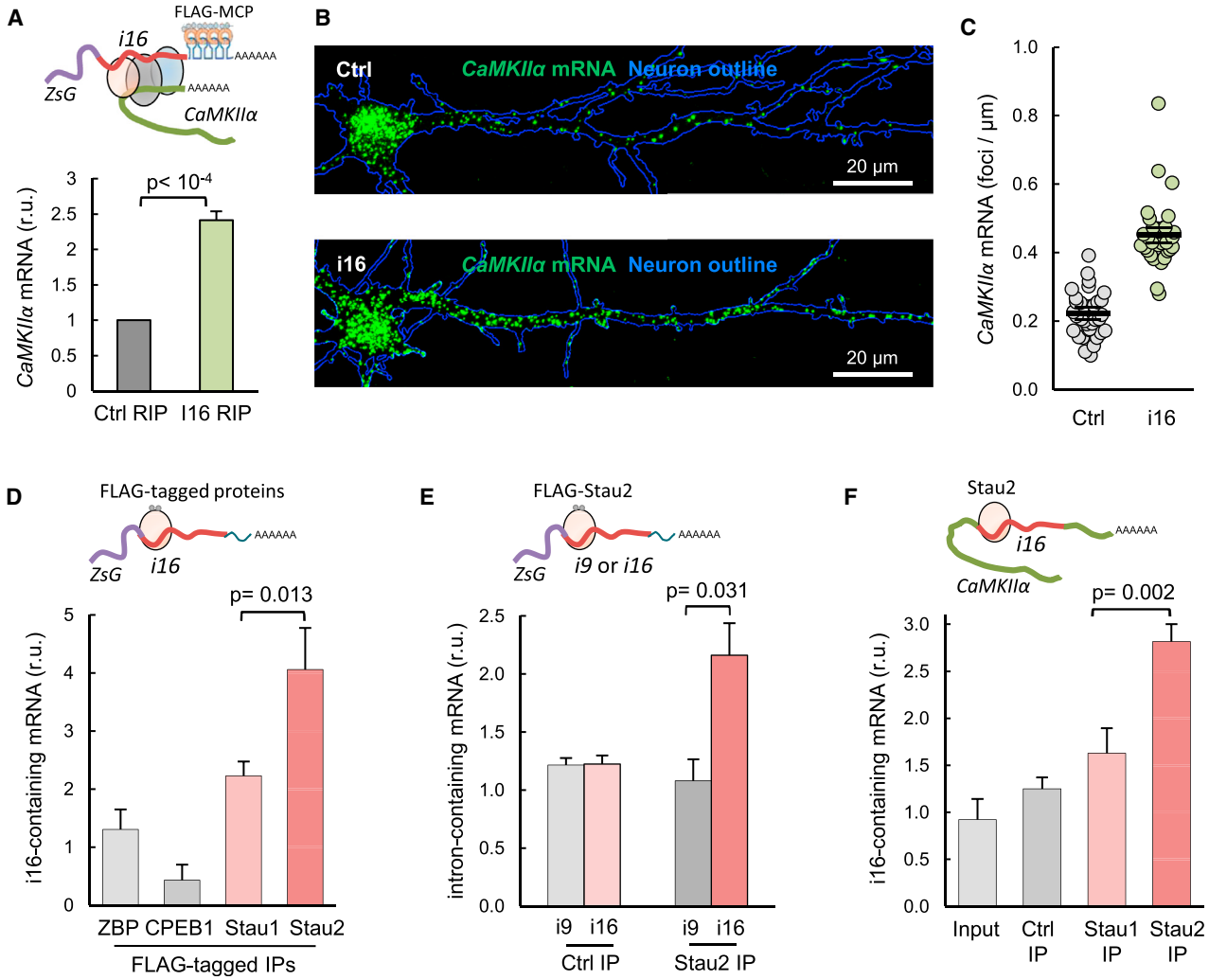

Figure 3. Intron i16 of *CaMKIIα* Interacts with Components of RNA Granules

(A) Neuro-2a cells were co-transfected with plasmids expressing FLAG-MCP and either 24× MBS fusions to ZsGreen-i16 or ZsGreen as control. FLAG immunoprecipitates (IPs) were used to quantify *CaMKIIα* mRNA levels by qRT-PCR against nonrelated *TBP* mRNA. Relative mean (n = 3) and SEM values are shown.

(B) Hippocampal neurons were co-transfected at 10 DIV with ZsGreen-i16 or ZsGreen as control, and GFP for neurite tracking. Cells were fixed 24 hr later and analyzed by FISH using only probes for exonic *CaMKIIα* mRNA.

(C) Quantification of (B). *CaMKIIα* mRNA foci per micrometer in 36 dendrites from 15 ZsGreen neurons and 33 dendrites from 14 ZsGreen-i16 neurons are plotted. Mean values (thick horizontal lines) and confidence limits (α = 0.05, thin horizontal lines) for the mean are shown.

(D) HEK293T cells were co-transfected with vectors expressing ZsGreen-i16 and FLAG-tagged Stau2, Stau1, CPEB1, or ZBP proteins. FLAG IPs were used to quantify ZsGreen-i16 mRNA enrichments over input by qRT-PCR. Nonspecific binding to the beads was corrected by measuring the levels of the nonrelated *TBP* mRNA. Relative mean (n = 3) and SEM values are shown. A representative western blot of Flag IPs is shown in Figure S3B.

(E) HEK293T cells were co-transfected with vectors expressing either ZsGreen-i16 or ZsGreen-i9 and Stau2-FLAG or empty vector as control. FLAG IPs were used to quantify ZsGreen-i16 and ZsGreen-i9 mRNA enrichment over input by qRT-PCR. Nonspecific binding to the beads was corrected by measuring the levels of the nonrelated *TBP* mRNA. Relative mean (n = 3) and SEM values are shown.

(F) Adult mice brain extracts (input) were immunoprecipitated with an anti-Stau2 antibody (Stau2 IP), anti-Stau1 antibody (Stau1 IP), or preimmune antisera (Ctrl IP) as control. Samples were used to quantify the enrichment levels over input of i16-containing *CaMKIIα* mRNA by qRT-PCR. Mean (n = 3) and SEM values are plotted. Input and IPs were analyzed by western blot to detect endogenous expression of Stau1 and Stau2 and IP efficiencies (see Figure S3C).

of Stau2 downregulation (Figure 4A) on nuclear and cytoplasmic i16 levels in short hairpin RNA (shRNA)-expressing cortical neurons. To monitor our subcellular fractionation procedures, we analyzed a nuclear mRNA (*Malat1*) and a cytoplasmic mRNA (*Gapdh*) (Figure S4A). As shown in Figure 4B, cytoplasmic i16-containing mRNA levels decreased significantly in Stau2-knockdown compared to control neurons. Notably, this decrease was not observed in nuclear samples, suggesting that Stau2 does not exert any effect on transcription or nuclear stability of i16-containing mRNA. To directly assess whether

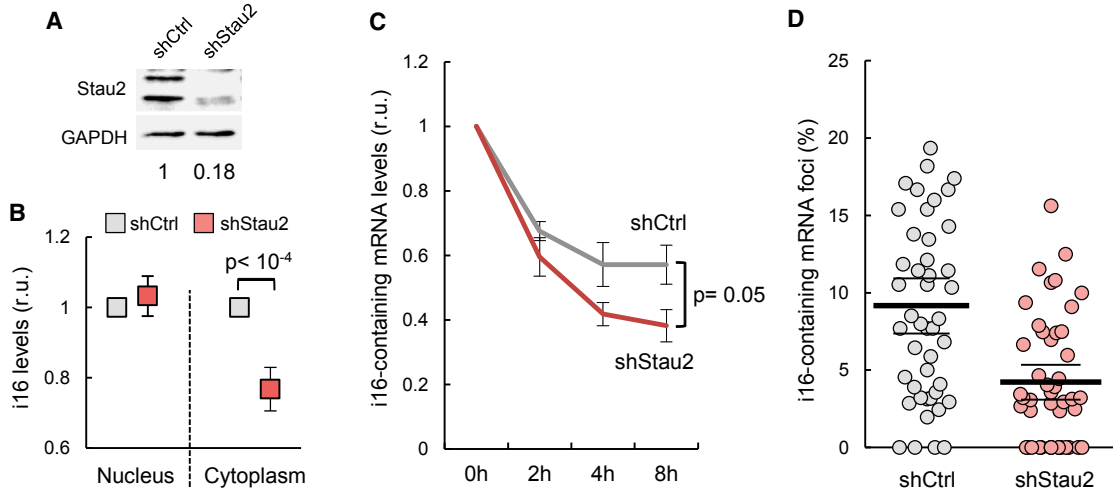

Figure 4. Stau2 Stabilizes and Increases Dendritic Levels of i16-Containing *CaMKIIα* mRNA

(A) Cortical neurons were infected at 3 DIV with lentiviral vectors expressing Stau2 (shStau2) or control (shCtrl) shRNAs and Stau2 levels were analyzed by western blot from cells collected at 14 DIV. GAPDH is shown as loading control.

(B) Cortical neurons as in (A) were used to obtain total RNA from nuclear and cytoplasmic fractions. Levels of i16-containing *CaMKIIα* mRNA were measured by qRT-PCR and compared with a non-retained intron. Relative mean values (n = 3) and SEM values are plotted.

(C) Neuro-2a cells were transfected with a vector expressing shStau2 or shCtrl, and RNA was isolated 48 hr post-transfection at the indicated times after actinomycin D (10 μg/ml) treatment. The stability of i16-containing *CaMKIIα* mRNA relative to control mRNA *eEF1A1* was measured by qRT-PCR. Relative mean (n = 3) and SEM values are plotted.

(D) Hippocampal neurons were infected at 3 DIV with lentiviral vectors expressing shStau2 or shCtrl, and *CaMKIIα* intron i16 and exonic sequences were detected by FISH as in Figure 2C at 14 DIV. Percentages of intronic relative to exonic foci in independent dendrites (n = 46) are plotted. Mean values (thick horizontal lines) and confidence limits (α = 0.05, thin horizontal lines) for the mean are also shown.

these changes in cytoplasmic RNA levels were a result of altered stability, we examined the half-life of i16-containing mRNA in Neuro-2a cells in which Stau2 was downregulated (shStau2). After transcriptional blockade with actinomycin D, i16-containing transcripts were significantly lower in shStau2-transfected cells than shCtrl-expressing cells (Figure 4C). In agreement with this result, the overexpression of Stau2 increased the stability of i16-containing mRNA (Figure S4B). To confirm the effect of Stau2 downregulation, we analyzed the presence of intron i16 in dendrites of hippocampal neurons by high-resolution FISH imaging and found that the percentage of i16-containing foci decreased by more than 50% under Stau2-knockdown conditions (Figure 4D). By contrast, we did not observe a significant downregulation of spliced *CaMKIIα* mRNA in the same samples (Figures S4C and S4D). Together, our results strongly suggest that Stau2 has a role in stabilizing and transporting i16-containing *CaMKIIα* mRNA in dendrites.

DISCUSSION

Our study provides new insights into the possible functions of intron retention in synaptic plasticity. Using two orthogonal approaches, we have demonstrated the presence of i16-containing *CaMKIIα* mRNAs in dendrites and synaptoneurosomes. Furthermore, we have found that intron i16 interacts with the RNA granule marker, Stau2 protein. Our data support the idea that the association between intron i16 and Stau2 enhances the dendritic localization of i16-containing *CaMKIIα* transcripts, likely through the assembly of these transcripts into RNA granules. New advances in RNP granule assembly mechanisms indicate that RNA could provide the local environment to polymerize different sets of proteins into a unique RNA granule for achieving its cellular fate. In this regard, our RIP experiments suggest that intron 16 and mature *CaMKIIα* mRNA would share common interacting proteins present in the same RNP particles. Stau2 could play such a role either by forming domain-swapping homodimers (Park and Maquat, 2013) or through indirect complex interactions within the same RNA granule. Interestingly, *CaMKIIα* mRNA has been found enriched in granules associated to low-complexity (LC) domain proteins from mouse brain (Han et al., 2012), supporting the idea that LC domains described in Stau proteins (Kato et al., 2012) could be important for RNP formation and dynamics.

Retained introns harbor sequences that may bind regulatory proteins to determine dendritic localization (Buckley et al., 2014). It is intriguing that the first 120 nt of intron i16 are strongly conserved between rodents and humans, which suggests that the 5′ end of intron i16 could be a target of specific proteins modulating its retention and/or localization. In this regard, the 5′ exon-intron boundary sequence of i16 is extremely rare compared to consensus sequences of U12- and U2- type introns (Turunen et al., 2013), and weak 5′ splice sites are typically characteristic of retained introns (Sakabe and de Souza, 2007).

Our results suggest a specific role for intron i16 in a subpopulation of *CaMKIIα* RNPs. In this regard, different BDNF mRNA splice variants are targeted to distinct cellular compartments (Baj et al., 2011), and only 10% of total *β-actin* mRNAs are actively transported to distal dendrites (Park et al., 2014), where

they show specific burst-like patterns of translation under stimulatory conditions (Wu et al., 2016).

We have found that i16-retained mRNA levels are downregulated upon synaptic stimulation in a translation-dependent manner. As it leads to increased *CaMKIIα* mRNA local translation (Aakalu et al., 2001), synaptic activation could trigger degradation of i16-containing mRNA by NMD, where indeed Stau2 could play a key role (Miki et al., 2011; Park and Maquat, 2013). Similarly to the regulation of Robo3 in axon guidance (Colak et al., 2013), synaptic stimulation would trigger a pioneer round of translation of the i16-contaning *CaMKIIα* mRNA and temporarily produce a protein isoform lacking the association domain, which would be particularly suitable for triggering a transient wave of diffusible *CaMKIIα* kinase activity at the synapsis (Stratton et al., 2014).

Another possibility is that intron i16 contains microRNA-response elements. Such elements could act as decoys or sponges in a manner similar to competitive endogenous RNA (Wong et al., 2016). Interestingly, components of the RNA-induced silencing complex (RISC) have been found in Stau2 RNA granules in dendrites (Fritzsche et al., 2013). Moreover, downregulation of MOV10, a key component of RISC, causes changes in the translation-active fraction of the *CaMKIIα* mRNA (Banerjee et al., 2009).

In summary, our data provide the first evidence of a specific interaction between a retained intron and the Stau2 protein to enhance dendritic localization of mRNAs. Given the important role of CaMKIIα in synaptic plasticity, our findings point to the idea that intron retention would add an additional layer of regulation to fine-tune CaMKIIα at synapses in both space and time for proper neuronal function.

EXPERIMENTAL PROCEDURES

Primary Neuron Cultures and Synaptoneurosomal Fractions

Dissociated mouse hippocampal and cortical neurons from E17.5 mice were cultured as described previously (Pedraza et al., 2014). See Supplemental Experimental Procedures for more information. Animal experimental procedures were approved by the ethics committee of the National Research Council of Spain (CSIC).

Quantitative and Semiquantitative RT-PCR

Methods used for quantitative and semiquantitative PCR have been described (Pedraza et al., 2014). All samples were treated with RNase-free DNase I (Thermo Scientific), and DNA contamination levels were assessed by qRT-PCR, omitting reverse transcriptase. In intronic disequilibrium analysis, qPCR results were corrected for primer efficiency using genomic DNA as template, and data were finally made relative to the intron with the lowest levels detected. A list of gene-specific primers can be found in Supplemental Experimental Procedures.

High-Resolution RNA In Situ Hybridization

Single-molecule mRNA detection was performed as described previously (Cajigas et al., 2012), with minor modifications (Supplemental Experimental Procedures). Signal quantification was performed using FociJ, a plugin with specific procedures that uses object libraries supplied in ImageJ (Wayne Rasband, NIH) to detect high-intensity foci as pixel groups markedly brighter compared to background. In addition to basic statistics on foci number, size, and brightness from different channels, this plugin provides with the minimal distances between foci and a neuronal tracking signal (usually a Map2 immunofluorescence field) to discard false positives. FociJ software is available upon request.

RNA Immunoprecipitation

RNA immunoprecipitation from cell extracts crosslinked with formaldehyde was performed as described previously (Moran et al., 2012). Further details are available in Supplemental Experimental Procedures.

SUPPLEMENTAL INFORMATION

Supplemental Information includes Supplemental Experimental Procedures and four figures and can be found with this article online at http://dx.doi.org/10.1016/j.celrep.2017.06.026.

AUTHOR CONTRIBUTIONS

Conceptualization, R.O. and C.G.; Investigation, R.O., M.V.G, S.G., N.P., and S.M.F-M.; Formal Analysis, R.O. and C.G.; Writing, C.G.; Funding Acquisition, C.G.

ACKNOWLEDGMENTS

We thank A. Cornadó, M. Kerexeta, and E. Rebollo for technical assistance, I. Cajigas for help on single-molecule FISH methods, and M. Kiebler for providing Staufen vectors and antibodies. We also thank M. Aldea, M. Kiebler, and J. Vilardell for helpful comments. This work was funded by grants from the Ministry of Economy and Competitiveness of Spain (BFU2014-52591-R CG) and the European Union (FEDER) to C.G.

Received: October 25, 2016
Revised: March 30, 2017
Accepted: June 8, 2017
Published: July 5, 2017

REFERENCES

Aakalu, G., Smith, W.B., Nguyen, N., Jiang, C., and Schuman, E.M. (2001). Dynamic visualization of local protein synthesis in hippocampal neurons. Neuron *30*, 489–502.

Baj, G., Leone, E., Chao, M.V., and Tongiorgi, E. (2011). Spatial segregation of BDNF transcripts enables BDNF to differentially shape distinct dendritic compartments. Proc. Natl. Acad. Sci. USA *108*, 16813–16818.

Banerjee, S., Neveu, P., and Kosik, K.S. (2009). A coordinated local translational control point at the synapse involving relief from silencing and MOV10 degradation. Neuron *64*, 871–884.

Bell, T.J., Miyashiro, K.Y., Sul, J.-Y., Buckley, P.T., Lee, M.T., McCullough, R., Jochems, J., Kim, J., Cantor, C.R., Parsons, T.D., and Eberwine, J.H. (2010). Intron retention facilitates splice variant diversity in calcium-activated big potassium channel populations. Proc. Natl. Acad. Sci. USA *107*, 21152–21157.

Braunschweig, U., Barbosa-Morais, N.L., Pan, Q., Nachman, E.N., Alipanahi, B., Gonatopoulos-Pournatzis, T., Frey, B., Irimia, M., and Blencowe, B.J. (2014). Widespread intron retention in mammals functionally tunes transcriptomes. Genome Res. *24*, 1774–1786.

Buchan, J.R. (2014). mRNP granules. Assembly, function, and connections with disease. RNA Biol. *11*, 1019–1030.

Buckley, P.T., Lee, M.T., Sul, J.Y., Miyashiro, K.Y., Bell, T.J., Fisher, S.A., Kim, J., and Eberwine, J. (2011). Cytoplasmic intron sequence-retaining transcripts can be dendritically targeted via ID element retrotransposons. Neuron *69*, 877–884.

Buckley, P.T., Khaladkar, M., Kim, J., and Eberwine, J. (2014). Cytoplasmic intron retention, function, splicing, and the sentinel RNA hypothesis. Wiley Interdiscip. Rev. RNA *5*, 223–230.

Buxbaum, A.R., Wu, B., and Singer, R.H. (2014). Single β-actin mRNA detection in neurons reveals a mechanism for regulating its translatability. Science *343*, 419–422.

Cajigas, I.J., Tushev, G., Will, T.J., tom Dieck, S., Fuerst, N., and Schuman, E.M. (2012). The local transcriptome in the synaptic neuropil revealed by deep sequencing and high-resolution imaging. Neuron *74*, 453–466.

Colak, D., Ji, S.-J., Porse, B.T., and Jaffrey, S.R. (2013). Regulation of axon guidance by compartmentalized nonsense-mediated mRNA decay. Cell *153*, 1252–1265.

Fritzsche, R., Karra, D., Bennett, K.L., Ang, F.Y., Heraud-Farlow, J.E., Tolino, M., Doyle, M., Bauer, K.E., Thomas, S., Planyavsky, M., et al. (2013). Interactome of two diverse RNA granules links mRNA localization to translational repression in neurons. Cell Rep. *5*, 1749–1762.

Han, T.W., Kato, M., Xie, S., Wu, L.C., Mirzaei, H., Pei, J., Chen, M., Xie, Y., Allen, J., Xiao, G., and McKnight, S.L. (2012). Cell-free formation of RNA granules: bound RNAs identify features and components of cellular assemblies. Cell *149*, 768–779.

Hell, J.W. (2014). CaMKII: claiming center stage in postsynaptic function and organization. Neuron *81*, 249–265.

Heraud-Farlow, J.E., and Kiebler, M.A. (2014). The multifunctional Staufen proteins: conserved roles from neurogenesis to synaptic plasticity. Trends Neurosci. *37*, 470–479.

Jeong, J.H., Nam, Y.J., Kim, S.Y., Kim, E.G., Jeong, J., and Kim, H.K. (2007). The transport of Staufen2-containing ribonucleoprotein complexes involves kinesin motor protein and is modulated by mitogen-activated protein kinase pathway. J. Neurochem. *102*, 2073–2084.

Kato, M., Han, T.W., Xie, S., Shi, K., Du, X., Wu, L.C., Mirzaei, H., Goldsmith, E.J., Longgood, J., Pei, J., et al. (2012). Cell-free formation of RNA granules: low complexity sequence domains form dynamic fibers within hydrogels. Cell *149*, 753–767.

Kiebler, M.A., and Bassell, G.J. (2006). Neuronal RNA granules: movers and makers. Neuron *51*, 685–690.

Miki, T., Kamikawa, Y., Kurono, S., Kaneko, Y., Katahira, J., and Yoneda, Y. (2011). Cell type-dependent gene regulation by Staufen2 in conjunction with Upf1. BMC Mol. Biol. *12*, 48.

Monshausen, M., Gehring, N.H., and Kosik, K.S. (2004). The mammalian RNA-binding protein Staufen2 links nuclear and cytoplasmic RNA processing pathways in neurons. Neuromolecular Med. *6*, 127–144.

Moran, V.A., Niland, C.N., and Khalil, A.M. (2012). Co-immunoprecipitation of long noncoding RNAs. Methods Mol. Biol. *925*, 219–228.

Park, E., and Maquat, L.E. (2013). Staufen-mediated mRNA decay. Wiley Interdiscip. Rev. RNA *4*, 423–435.

Park, H.Y., Lim, H., Yoon, Y.J., Follenzi, A., Nwokafor, C., Lopez-Jones, M., Meng, X., and Singer, R.H. (2014). Visualization of dynamics of single endogenous mRNA labeled in live mouse. Science *343*, 422–424.

Pedraza, N., Ortiz, R., Cornadó, A., Llobet, A., Aldea, M., and Gallego, C. (2014). KIS, a kinase associated with microtubule regulators, enhances translation of AMPA receptors and stimulates dendritic spine remodeling. J. Neurosci. *34*, 13988–13997.

Sakabe, N.J., and de Souza, S.J. (2007). Sequence features responsible for intron retention in. BMC Genomics *8*, 59–72.

Stratton, M., Lee, I.H., Bhattacharyya, M., Christensen, S.M., Chao, L.H., Schulman, H., Groves, J.T., and Kuriyan, J. (2014). Correction: activation-triggered subunit exchange between CaMKII holoenzymes facilitates the spread of kinase activity. eLife *3*, e02490.

Tang, S.J., Meulemans, D., Vazquez, L., Colaco, N., and Schuman, E. (2001). A role for a rat homolog of staufen in the transport of RNA to neuronal dendrites. Neuron *32*, 463–475.

Turunen, J.J., Niemelä, E.H., Verma, B., and Frilander, M.J. (2013). The significant other: splicing by the minor spliceosome. Wiley Interdiscip. Rev. RNA *4*, 61–76.

Ule, J., and Darnell, R.B. (2006). RNA binding proteins and the regulation of neuronal synaptic plasticity. Curr. Opin. Neurobiol. *16*, 102–110.

Wong, J.J.L., Ritchie, W., Ebner, O.A., Selbach, M., Wong, J.W.H., Huang, Y., Gao, D., Pinello, N., Gonzalez, M., Baidya, K., et al. (2013). Orchestrated intron retention regulates normal granulocyte differentiation. Cell *154*, 583–595.

Wong, J.J.L., Au, A.Y.M., Ritchie, W., and Rasko, J.E.J. (2016). Intron retention in mRNA: No longer nonsense: Known and putative roles of intron retention in normal and disease biology. BioEssays *38*, 41–49.

Wu, B., Eliscovich, C., Yoon, Y.J., and Singer, R.H. (2016). Translation dynamics of single mRNAs in live cells and neurons. Science *352*, 1430–1435.

Yap, K., Lim, Z.Q., Khandelia, P., Friedman, B., and Makeyev, E.V. (2012). Coordinated regulation of neuronal mRNA steady-state levels through developmentally controlled intron retention. Genes Dev. *26*, 1209–1223.

Cell Reports, Volume *20*

Supplemental Information

Recruitment of Staufen2 Enhances Dendritic Localization of an Intron-Containing *CaMKIIα* mRNA

Raúl Ortiz, Maya V. Georgieva, Sara Gutiérrez, Neus Pedraza, Sandra M. Fernández-Moya, and Carme Gallego

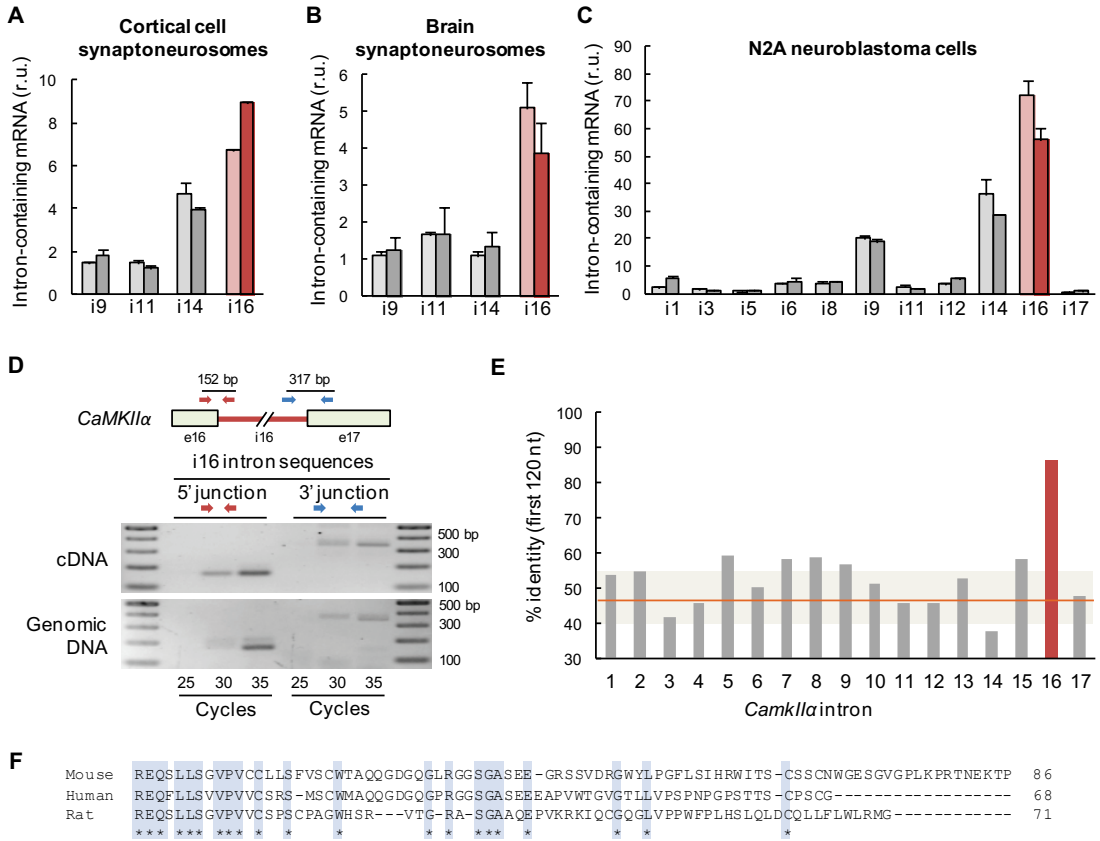

Figure S1, related to Figure 1. *CaMKIIα* intron disequilibrium analysis. RNA samples obtained from cultured cortical-cell Percoll-gradient synaptoneurosomes (A), total-brain Percoll-gradient synaptoneurosomes (B) and N2A cells (C) were analyzed to quantify exon-intron junction levels by qRT-PCR as in Figure 1. Each bar corresponds to an independent experiment and represents the relative mean value from three independent qRT-PCR Ct measurements. Confidence limits (α=0.05) are also shown. (D) Scheme of intron i16 *CaMKIIα* mRNA and adjacent exons showing primers used for semi-quantitative PCR analysis of cDNA from mouse nucleus-free brain extracts. Primer efficiency was assessed by genomic DNA amplification. (E) Level of similarity of the first 120 nt of mouse, human and rat CaMKIIα introns. (F) Amino acid sequence alignment of translated CaMKIIα intron sequences in Figure 1F.

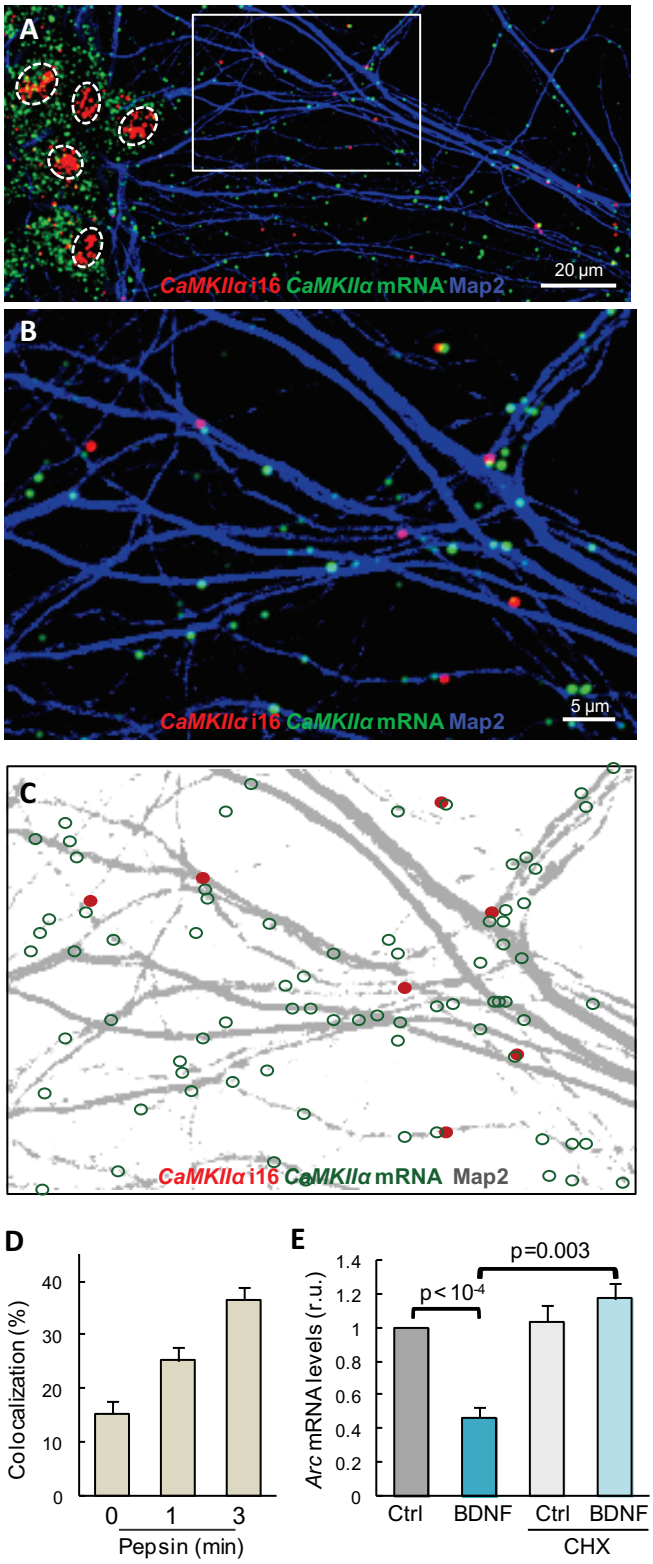

Figure S2, related to Figure 2. Single-molecule analysis of i16-containing *CaMKIIα* mRNA in hippocampal neurons. (A, B) 14 DIV hippocampal cells were analyzed by FISH using custom *View*RNA probes against intron i16 (red) or exonic (green) *CaMKIIα* sequences. Dendrites were decorated with an αMap2 antibody (blue). (C) Outline of identified foci in the red and green channels with the aid of FociJ. (D) Co-localization percentages of intronic (n>1000) to exonic foci were measured in neurons treated for different times with 100 µg/ml pepsin. Confidence limits (α=0.01) are also indicated. (E) Cortical cell cultures (18 DIV) were treated with actinomycin D (10 µg/ml) for one hour prior to stimulation with BDNF 200 ng/ml or vehicle for 30 min. Where indicated, cycloheximide was added to 25 µg/ml 5 min before BDNF. After stimulation, synaptoneurosomal fractions were obtained by filtration and used to quantify *Arc* mRNA levels relative to *Gapdh* mRNA by qRT-PCR. Relative mean (n=3) and SEM values are shown.

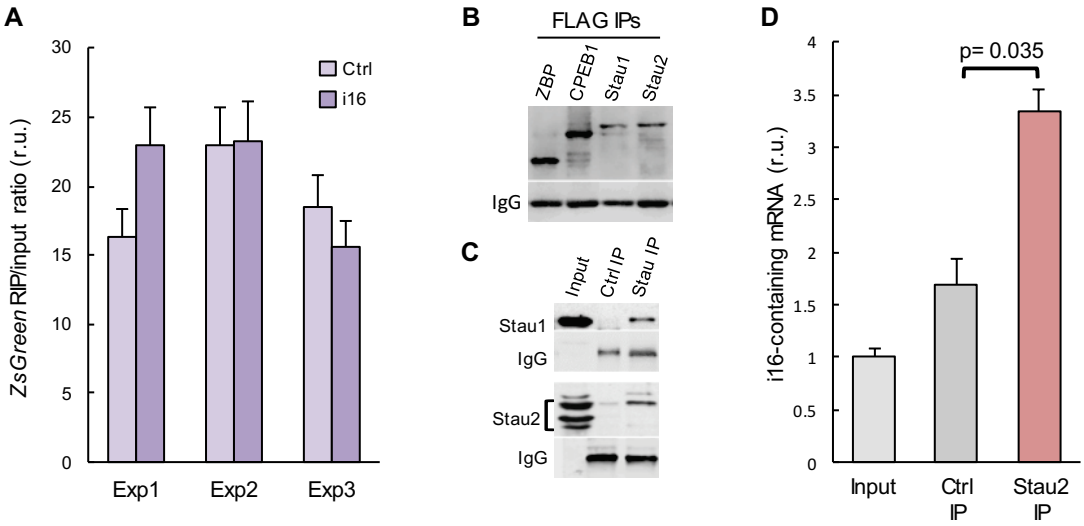

Figure S3, related to Figure 3. *CaMKIIα* intron i16 enrichment in RNA-immunoprecipitation assays.
(A) Samples from ZsGreen-i16 or control transfected Neuro-2a cells analyzed in Figure 3A were used to quantify ZsGreen and obtain RIP/input ratios. Relative mean values from qRT-PCR replicates (n=3) are shown for three independent experiments. Confidence limits (α=0.05) for the mean are also indicated.
(B) Related to Figure 3D, a representative western blot of FLAG immunoprecipitates (IP) from HEK293T cells co-transfected with vectors expressing ZsGreen-i16 and FLAG tagged Stau2, Stau1, CPEB1 and ZBP proteins.
(C) Related to Figure 3F, representative western blot of Stau1 and Stau2 endogenous levels in extracts and IPs.
(D) Cultured cortical cells (18 DIV) were immunoprecipitated with an anti-Stau2 antibody (Stau2 IP) or preimmune antisera (Ctrl IP) as control. Samples were used to quantify the enrichment levels over input of i16-containing *CaMKIIα* mRNA by qRT-PCR. Relative mean values from qRT-PCR replicates (n=3) and confidence limits (α=0.05) are shown.

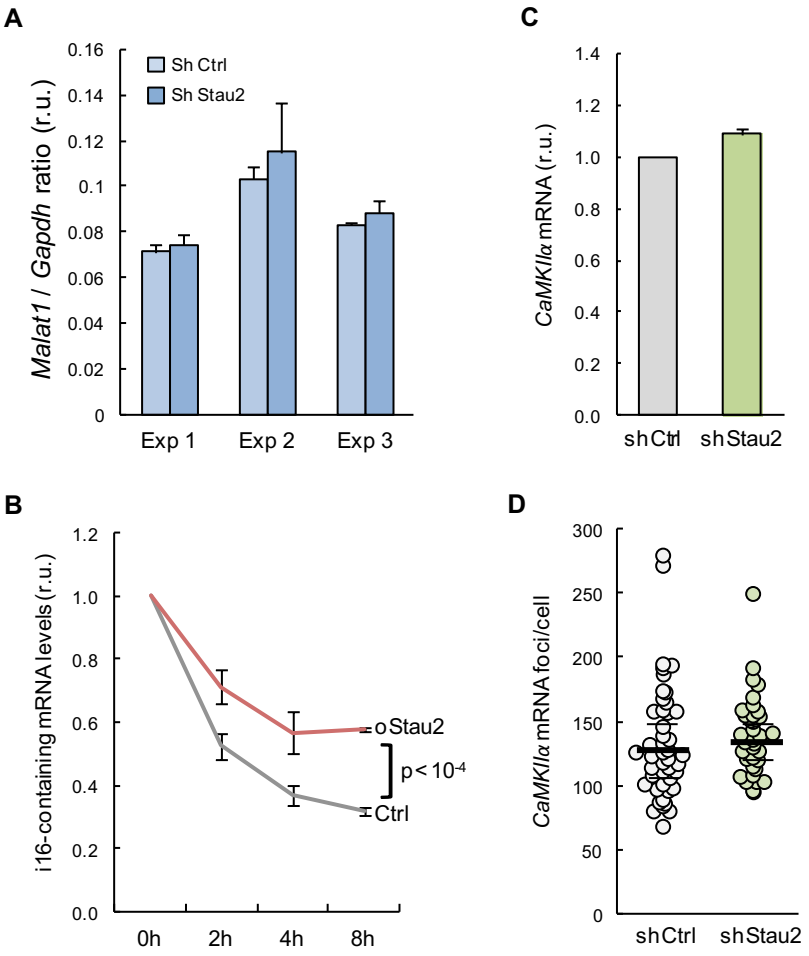

Figure S4, related to Figure 4. (A) Subcellular fractions from cortical neurons expressing shStau2 or shCtrl analyzed in Figure 4B were used to measure levels of *Malat1* (as mainly nuclear) and *Gapdh* (as mainly cytoplasmic) mRNAs. Bars correspond to cytoplasmic versus nuclear *Malat1/Gapdh* ratios. Mean ratios and SEM values from qRT-PCR replicates (n=3) are shown for three independent experiments. (B) Neuro-2a cells were transfected with Stau2 or GFP as control, and RNA was isolated 24 h post-transfection at indicated times after actinomycin D (10 µg/ml) treatment. The stability of i16-containing mRNA was measured by qRT-PCR relative to control *eEF1A1* mRNA. Relative mean (n=3) and SEM values are plotted. (C) *CaMKIIα* mRNA levels relative to *Gapdh* mRNA were obtained by RT-qPCR from same samples as in Figure 4B. Relative mean values (n=3) and SEM values are shown. (D) Related to Figure 4D, *CaMKIIα* mRNA levels were measured by FISH in ShCtrl or ShStau2 infected hippocampal cultures and foci numbers per cell are plotted. Mean values (thick horizontal lines) and confidence limits (α=0.05, thin horizontal lines) for the mean are also shown.

Supplemental Experimental Procedures

Primary neuron cultures. Cells were plated at 10^5 cells/cm^2 for biochemistry experiments and 1-2x10^4 cells/cm^2 for imaging experiments. Neuron transfection and lentivirus production protocols were as described (Pedraza et al., 2014). Lentiviruses encoding Stau2 and scrambled shRNAs were kind gifts from M. Kiebler. For imaging neuronal dendrites and cell bodies separately, PDMS microfluidic chambers (AX50010 AXIS™ Axon Isolation Device, 500 µm, Millipore) were placed onto cover glasses coated with poly-L-lysine and neurons were then plated with 5 µl/well at 5x10^6 neurons/ml (Taylor et al., 2010). In this device neurons are loaded into a channel with a set of microgrooves whose dimensions (approximately 5 µm in height by 10 µm in width) are selected because they prevent cell bodies from flowing through while allowing passage to dendrites and axons. As microgroove lenght is 500 µm, dendrites can extend completely.

Preparation and stimulation of functional synaptoneurosomes by Percoll gradient. Synaptoneurosomes were obtained as previously described (Nagy and Delgado-Escueta, 1984), with some modifications. Synaptoneurosomes were obtained from cultured cortical neurons (14 DIV) or adult mice cortex (~5 weeks). Prior to homogenization, cultured neurons were collected with a cell scrapper, while brain cortex was chopped into small pieces in ice-cold homogenization buffer (0.32 M sucrose, 1 mM EDTA, 1 mg/ml BSA, 5 mM HEPES pH 7.4 in DEPC-treated water). Tissue was then homogenized with the aid of a glass-teflon douncer, with 10 strokes at 650 rpm. The homogenate (crude extract, CE) was centrifuged at 3000g for 10 min to remove cell debris, yielding P1 and S1, this supernatant was centrifuged again at 14000g for 12 min. The pellet was resuspended in Krebs HEPES buffer (150 mM HCl, 3 mM KCl, 10 mM glucose, 2 mM $MgSO_4$, 2 mM $CaCl_2$, 10 mM HEPES pH 7.4), and Percoll was added to 45% v/v and mixed carefully by inverting the tube. After spinning samples for 2 min at 14000 g, synaptoneurosomes were recovered from the upper layer, washed once in Krebs HEPES buffer and centrifuged again for 30 sec at 14000g. The final pellet containing synaptoneurosomes (Syn) was resuspended in Krebs HEPES buffer to 1µg/µl for stimulation. Synaptoneurosomes were incubated for 30 min at 37ºC in BDNF (100 ng/µl) or NMDA (50 µg/ml).

Cortical neurons stimulation and obtention of synaptoneurosomal fraction by filtration. Primary cortical cultures (18 DIV) were treated with actinomycin D (10 µg/ml) for 1h before stimulation to avoid any possible transcriptional effect. Selected plates were stimulated for 30 min with BDNF (200 ng/ml) and, where indicated, cycloheximide (25 µg/ml) was applied 5 min prior BDNF stimulation. After culture treatment, plates were washed twice in ice-cold PBS-MC (1xPBS supplemented with 1 mM magnesium chloride and 0.1 mM calcium chloride). Neurons were collected with a cell scrapper in homogenization buffer (118 mM NaCl, 4.7 mM KCl, 1.2 mM MgSO4, 2.5 mM CaCl2, 1.53 mM KH2PO4, 212.7 mM glucose, 1 mM DTT, pH 7.4, protease and phosphatase inhibitors and 40 U/ml RNase inhibitor). Collected cells were homogenated by four gentle strokes in a glass-teflon douncer on ice. Homogenate was passed two times through 100 µm nylon mesh filters (Millipore) and two times through a 5 µm PVDF membrane (Millipore). Filtrate was centrifuged at 1000 g for 10 min at 4ºC and RNA was obtained from synaptosomal containing pellet using TRI reagent (Sigma). RNA was analyzed by RT-qPCR. *Gapdh* mRNA was used to normalize samples.

RNA immunoprecipitation. Cells were collected by trypsinization and, when required, treated with 0.3% formaldehyde for 10 min and quenched with 0.125 M Glycine. After a washing step, samples were resuspended in RIP buffer (DEPC-treated water containing 20 mM HEPES pH 7.4, 150 mM NaCl, 1 mM $MgCl_2$, 0.1% Triton X-100, 10% glycerol, 0.5 mM DTT, 1× protease inhibitor cocktail (Roche), and 40 U/ml RNase inhibitor), sonicated and centrifuged at 10000 g for 10 min to remove cell debris. Supernatants were then incubated with anti-FLAG M2 beads (Sigma) for 4 h at 4ºC and, after washing steps, RNA was collected in TRK buffer (E.Z.N.A. total RNA Kit I; Omega Bio-Tek). Endogenous *CaMKIIα* or reporter *ZsGreen* mRNA levels in IPs were made relative to input to correct for differences in extract concentration between conditions. Unspecific binding to beads was corrected by measuring the levels of *TBP* as non-related mRNAs.
For endogenous RNA immunoprecipitation from brain, tissue was homogenated using a glass-teflon douncer and, as we were interested in cytoplasmatic interactions, homogenate (Crude extract, CE) was centrifuged at 1000g for 10 min and supernatant was centrifuged again at 10000g for 10 min. This second supernatant (S2) was used as input for the IP and checked for nucleus contamination by western blot as in Figure 1D. Input samples were pre-cleared with protein A beads (Protein A Sepharose CL-4B, GE Healthcare) and sequentially incubated with αStau1or αStau2 antibodies (M. Kiebler) or a control IgG for 3 h, and protein A beads for 1h. Endogenous i16 containing *CaMKIIα* mRNA in IPs and unspecific binding to beads were made relative to the other introns.

Preparation of RNA granules from brain. We followed essentially a published protocol (Cambray et al., 2009). Briefly, brains were homogenized in IMAC buffer (20 mM HEPES, pH 7.4, 140 mM potassium acetate, 1 mM magnesium acetate, 1 mM EGTA, protease and phosphatase inhibitors and 40 U/ml RNase inhibitor). The homogenate was fractionated by successive centrifugation steps to yield the indicated pellets (P) and supernatants (S). Total extracts were centrifuged at 1000 g for 10 min, giving rise to S1 and P1. The S1 supernatant was centrifuged at 10000 g for 10 min, yielding S2 and P2. The S2 supernatant was centrifuged at 100000 g for 1 h, resulting in S3 and RNA granules containing pellet P3.

High-resolution RNA in situ hybridization. Single-molecule mRNA detection was performed as described (Cajigas et al., 2012) with probes targeting first 800 nt of intron 16 (intronic probe) and exons 3-16 of spliced CamKIIα mRNA (exonic probe). We routinely controlled the nonspecific signal by using an unrelated probe (ZsGreen) as dummy or omitting the probe. FISH procedures were done following the manufacturer's instructions with some modifications. Briefly, 14 DIV hippocampal cells were fixed in 4% p-formaldehyde and 4% sucrose for 30 min at 4ºC. As we wanted to combine this procedure with Map2 immunofluorescence, hybridizations were performed without previous proteinase K treatment. For colocalization experiments only, cultures were treated with 100 µg/ml pepsin (Sigma) for 1 to 3 min (Buxbaum et al., 2014). When required, immunofluorescence was performed for cell tracking purposes with anti-Map2 (M1406, Sigma) or Alexa488-labeled anti-GFP (A21311, ThermoFisher Scientific) antibodies (1:500 dilution). Images were acquired with a Zeiss LSM780 confocal microscope as 30-image 0.5 µm stacks under a 63×objective at 0.13 µm/pixel.

Miscellaneous. Nuclear and cytoplasmic fractions from cells and cortical cells were obtained as described (Niblock et al., 2016). Western blot analysis (Pedraza et al., 2014) was carried out with antibodies αFLAG (1:1000 dilution, F3165, Sigma), αStau1 (1:500 dilution, M. Kiebler), αStau2 (1:500 dilution, M. Kiebler), αPSD-95 (1:2000 dilution, #MABN68, EMD Millipore), αHistone H3 (1:2000 dilution, ab1791, Abcam), and αhnRNPA2/B1 (1:1000, NB120-6102, Novus Biologicals). To avoid interference from IgG used in IPs, HRP-labeled protein A/G was used (ref 32490, ThermoFisher Scientific) at 1:10000 dilution. Details of all DNA constructs used are available upon request.

Primers used for quantitative PCR:

Target	Type	Sequence 5' - 3'
CaMKIIα exon 1 - intron 1	Forward	CCCGATTCACAGAAGAGTA
	Reverse	CCATGCTCTCTAGGACTC
	Probe	TTTGAGGAACTGGGAAAGTGAGTCA
CaMKIIα exon 2 - intron 2	Forward	TGCCAAGATTATCAACAC
	Reverse	AGGGTCTATTCTCTTCAC
	Probe	CAGCCAGAGGTAGGTTACCGCAC
CaMKIIα intron 3 - exon 4	Forward	GTTGCTCCTGGAATTTAAC
	Reverse	CGAAGATAAGGTAGTGGTG
	Probe	ATGACAGCATCTCCGAGGAGG
CaMKIIα exon 5 - intron 5	Forward	GGAACTGTTTGAAGACATTG
	Reverse	CTGGGAAGCTGACTGTAG
	Probe	TGAGTACTGGCTGCAACCTGG
CaMKIIα exon 6 - intron 6	Forward	GACCTGAAGGTGAGTAAC
	Reverse	GGTGGAGACATGAAAGAA
	Probe	AAGCAGCTTTCCCAAGTCCC
CaMKIIα exon 8 - intron 8	Forward	CTGTGGTAAGTCCAATCC
	Reverse	CAGGAGAGGAGAGATGAC
	Probe	AGCCCTGTTCGTCTCCCAGC
CaMKIIα exon 9 - intron 9	Forward	GTACCAGCAGATCAAAGC
	Reverse	AGACCCTAATCACTAGGC
	Probe	CCTATGATGTGAGTGTTGCTCCC
CaMKIIα exon 10 - intron 10	Forward	TCGGTGAGCCTTTATCAG
	Reverse	CAGTGAGCCAGAGATTCC
	Probe	CGTGCTCCTCCAGGTCTTGT
CaMKIIα exon 11 - intron 11	Forward	GCCTGAAGAAGTTCAATG
	Reverse	AACCGATGAAGAGAAGAG
	Probe	AACTGAAGGTAACCTGTCCTTATTCCT
CaMKIIα exon 12 - intron 12	Forward	CCATCCTCACCACTATGC
	Reverse	GCTACCCAACAGTGTAATG
	Probe	CCACCAGGAACTTCTCCGGT
CaMKIIα intron 14 - exon 15	Forward	CTGTCGTTATTTGTGTCC
	Reverse	GACTCAAAGTCTCCATTG
	Probe	CTACCTTACAGTGCGCAAACAG

CaMKIIα exon 15 - intron 15	Forward	ACAGGAAATTATCAAAGTGA
	Reverse	GAGTGAGTAGGTTCAGAA
	Probe	AGCTGATCGAAGCCATAAGCAAT
CaMKIIα exon 16 - intron 16	Forward	CCTGGACTTTCATCGATTC
	Reverse	GAGAGCAGACAACAGACA
	Probe	ATTTTGAAAACCGTGAGCAATCCCT
CaMKIIα exon 17 - intron 17	Forward	TCCACTTCCACAGATCTG
	Reverse	CCTCTACTAAGGCAATACC
	Probe	TCCTGCCGCAGTAAGGATTCT
CaMKIIα	Forward	GACGAAGACACCAAAGTG
	Reverse	GGACTCAAAGTCTCCATTG
	Probe	ACAGGAAATTATCAAAGTGACAGAGC
eEF1A1	Forward	GAGCCAAGTGCTAATATG
	Reverse	TGGTGGTAGGATACAATC
	Probe	AAAGTCACCCGCAAAGATGGC
Gapdh	Forward	GGTCTACATGTTCCAGTA
	Reverse	CCCATTTGATGTTAGTGG
	Probe	ATTCAACGGCACAGTCAAGGC
Malat1	Forward	GTGCTGAAAATTAGATGTTC
	Reverse	CCTTCTAAATACATACATTCTCTA
	Probe	AATGTGCTCCAATGTACTTGTGCTT
ZsGreen	Forward	GTGGAGGAGAACTGCATG
	Reverse	TGTCGGTCATCTTCTTCA
	Probe	ACCACGAGTCCAAGTTCTACGG
TBP	Forward	CACCAATGACTCCTATGA
	Reverse	CCAAGATTCACGGTAGATA
	Probe	CCTATCACTCCTGCCACACCA
CdkN1a	Taqman	Hs00176828_m1

Semiquantitative PCR primers

Target	Type	Sequence 5' - 3'
CaMKIIα long isoform ENSMUST00000102888.9	Forward	CCATCCTCACCACTATGC
	Reverse	CTGGATCTTCCTTCTTCAC
CaMKIIα short isoform ENSMUST00000039904.6	Forward	CTTGCCTGGTGTTGCTAA
	Reverse	CTGGATCTTCCTTCTTCAC
Exon16 - Intron16 junction	Forward	CCTGGACTTTCATCGATTC
	Reverse	CTGGATCTTCCTTCTTCAC
Intron16 - Exon17 junction	Forward	TGTGGTATCCTGTTATCTAG
	Reverse	CCATCAGGTGGATGTGAG

Supplemental References

Cambray, S., Pedraza, N., Rafel, M., Garí, E., Aldea, M. and Gallego, C. (2009).Protein kinase KIS localizes to RNA granules and enhances local translation. Mol Cell Biol. *29*, 726-735.

Nagy, A., Delgado-Escueta, A.V. 1984. Rapid preparation of synaptosomes from mammalian brain using nontoxic isoosmotic gradient material (Percoll). J Neurochem. *43*, 1114-1123.

Niblock, M. et al. (2016). Retention of hexanucleotide repeat-containing intron in C9orf72 mRNA: implications for the pathogenesis of ALS/FTD. Acta Neuropathol Commun. *4*, 18.

Taylor, A.M., Dieterich, D.C., Ito, H.T., Kim, S.A. and Schuman, E.M. (2010). Microfluidic local perfusion chambers for the visualization and manipulation of synapses. Neuron *66*, 57-68.